NANOSYSTEMS: PHYSICS, CHEMISTRY, MATHEMATICS, 2014, 5 (5), P. 692–702

SYNTHESIS AND THE STUDY OF MAGNETIC CHARACTERISTICS OF NANO $La_{1-x}Sr_xFeO_3$ BY CO-PRECIPITATION METHOD

A. T. Nguyen[1], M. V. Knurova[2], T. M. Nguyen[3], V. O. Mittova[4], I. Ya. Mittova[5]

[1]Ho Chi Minh City Pedagogical University, Ho Chi Minh City, Viet Nam

[2]Voronezh State University, Voronezh, Russia

[3]Ha Noi National University of Education, Ha Noi, Viet Nam

[4]Voronezh State Medical Academy, Voronezh, Russia

[5]Voronezh State University, Voronezh, Russia

anhtien0601@rambler.ru, cnurova2010@yandex.ru, montvn@gmail.com, vmittova@mail.ru, imittova@mail.ru

PACS 75.50.Cc, 81.07.Wx

The goal of this study was the sol-gel synthesis of nanocrystals $La_{1-x}Sr_xFeO_3$ (x=0.0, 0.1, 0.2, 0.3) and an examination of their magnetic properties. An aqueous solution of ammonia and 5% ammonium carbonate solution were used as precipitating agents. It was established that the crystallization of $LaFeO_3$ is completed at 750°C (annealing for 1 h). The average diameter of the synthesized particles was 80–100 nm. Investigation of the magnetic properties showed non-monotonic changes of saturation magnetic moment and increase of coercive force with increased Sr content in the sample.

Keywords: sol-gel synthesis; nanopowders; lanthanum ferrite; magnetic properties; high-coercivity materials.

Received: 28 August 2014
Revised: 13 October 2014

1. Introduction

In the late 1980's, nanotechnology began to develop and achieved many great improvements not only in research but also in many applications. Nanomaterials and nanotools exhibit new physical and chemical effects and properties that do not exist in bulk materials with the same chemical composition [1].

Materials widely used in practice are magnetic materials and other functional materials, which are applied to various electronic devices such as transformers, generators, electric motors, digital detectors, voice recorder, video recorder, etc. These materials, having ABO_3-typed perovskite-like structure (where A is a such as Y, La, Ln (rare earth metals), Bi and B is transition metal such as Mn, Fe, Co , Ni, Cr), are studied intensively due to their outstanding properties and difficult synthesis [5-11]. These materials are also studied as catalysts [12].

Modified ABO_3 compounds are materials where A or B or both A and B ions are partially replaced by other metal ions (such as Ca, Sr, Cd, Ln (rare earth metals), Mn, Fe, Ni, Al, etc.) [13-17]. This modification produces mixed-valence state of metals and structural defects, which create more interesting effects such as thermal effects, thermomagnetic effects, and large magnetoresistance for material substrate. That has opened up new application of

perovskite materials in a number of modern industrial areas such as electronics, information, petro-chemical processing technologies.

Currently, in order to prepare ABO_3-typed perovskite materials with small particle size, various basic methods are commonly used, such as co-precipitation at room temperature, sol-gel method, co-complexing method, etc. The advantage of these methods is that the crystallization process occurs at lower temperatures than that of traditional ceramic synthesis and the obtained composite materials have more uniform compositions with higher purity. However, to synthesize nanosized ABO_3 materials via these methods, it is required to investigate many factors affecting the formation of the single-crystalline phase such as temperature, calcination time, pH, gelling substance/metal molar ratio, gelling temperature, etc. This investigation requires much time and effort.

Currently, much attention is being devoted to the investigation of the particle size, structure and properties of substituted ferrite. In particular, [15] it was shown that the doping of yttrium ferrite by calcium leads to a reduction of particle size from 50 nm to 27.5 nm, an increase of magnetization (J) from 0.070 to 0.148 Am^2/kg and a decrease in the coercive force (H_c) from 3.58 to 2.78 kA/m in a field of 640 kA/m. The fact that the doping of cobalt ferrite with zinc leads to increased magnetization from 71.297 Am^2/kg for $CoFe_2O_4$ up to 152.531 Am^2/kg for $Co_{0.5}Zn_{0.5}Fe_2O_4$ was demonstrated [18].

However, the synthesis of nano $La_{1-x}Sr_xFeO_3$-typed perovskite materials by hydrolysis of metal cations in boiling water and the addition of a solution containing a precipitating agent and the study of magnetic characteristics of the synthesized material have not been reported.

In this study, nano $La_{1-x}Sr_xFeO_3$-typed perovskite materials (x = 0.0, 0.1, 0.2 and 0.3) were synthesized using the co-precipitation method in boiling water and studied their magnetic properties.

2. Materials and methods

The chemicals used in the research were analytically pure: $Fe(NO_3)_3{\cdot}9H_2O$, $La(NO_3)_3{\cdot}6H_2O$, $Sr(NO_3)_2$, 25% NH_3, $(NH_4)_2CO_3$. The salts were dissolved in water with the concentration of 0.15M. Precipitating agents used in the experiments were aqueous ammonia and ammonium carbonate in 15% excess as compared to the amount in stoichiometry equation to ensure the complete precipitation of metal ions in the solution.

Many studies demonstrate that sols of iron and lanthanum oxides, and a mixture of sols of iron (III) and lanthanum oxides can be obtained by co-precipitation of Fe^{3+} and La^{3+} in boiling water [11, 19, 20]. The results of a previous study [11] demonstrated that use of the co-precipitation is the optimal method.

Nano $La_{1-x}Sr_xFeO_3$ materials were synthesized by adding an aqueous solution containing $La(NO_3)_3$, $Sr(NO_3)_2$ and $Fe(NO_3)_3$ drop wise into boiling water with the molar ratio La : Sr : Fe = (1- x) : x : 1 and x = 0.0, 0.1, 0.2, 0.3 with magnetic stirring. The solution was boiled for 5 minutes and then cooled down to room temperature. Then, 5% ammonia solution (for x = 0.0) and 5% ammonium carbonate (x = 0.1, 0.2, 0.3) were slowly added into the obtained solution with concurrent vigorous stirring for about 30 minutes. The obtained precipitate was separated using vacuum filter, washed with distilled water before being dried naturally at room temperature. The obtained powder was finely ground then calcined in air at different temperatures: 750, 850 and 950°C to examine the completion of crystallization process and the formation of homogeneous phase.

The physicochemical processes, occurring when heating the samples, were studied by DTA/TGA method performed on a TGA Q500 V20.13 Build 39, with a maximum temperature of 1100°C and heating rate of 10°C/min.

The phase composition of obtained powder was examined by X-ray diffraction method on a D8-ADVANCE.

Elemental composition of the samples was tested by the method of energy-dispersive X-ray spectroscopy (EDXS, INCA Energy-250) and atomic absorption spectroscopy according to the reference of Ref. AOAC 965.09 (ICE-3500).

The size and shape of particles were determined by scanning electron microscope (SEM, JE-1400).

The magnetic characteristics (saturation magnetization, remanent magnetization, coercive force) of the material were determined on vibrating sample magnetometers Microsene EV11, performed at room temperature.

3. Results and discussion

3.1. $LaFeO_3$ nano-materials synthesis results

Fig. 1 shows TGA diagram of powder sample (with x = 0.0) dried naturally at room temperature.

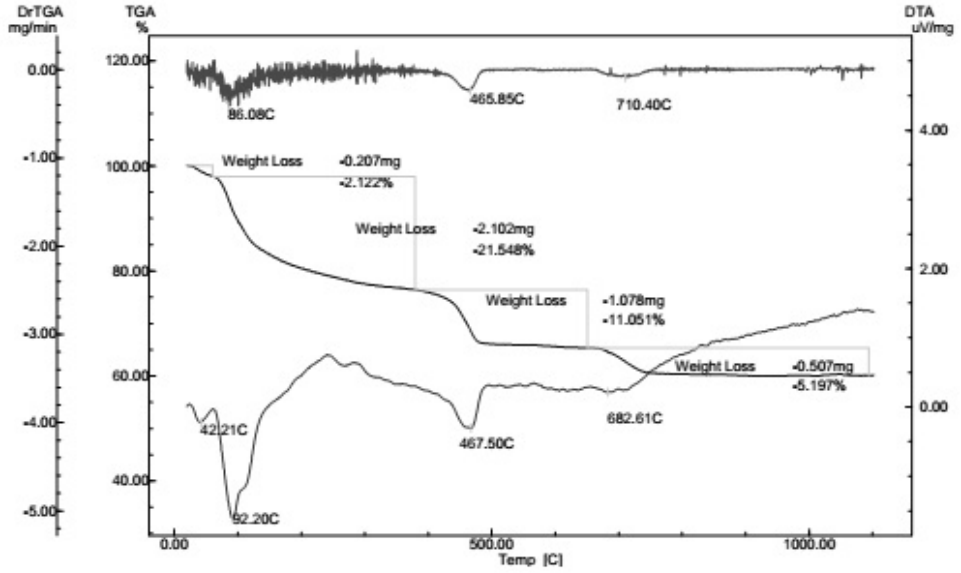

Fig. 1. TGA/DTA diagram of powder sample

It can be seen from Fig. 1 that the TGA curve exhibited 3 weight loss effects with a total weight loss of about 40%. The first weight loss period occurred from room temperature to 370°C with the weight loss of 23.67% corresponding to an endothermic peak at 92.20°C and a small peak at 42.21°C, which was attributed to the loss of surface water, desorption, and the dehydration of iron(III) hydroxide to from FeOOH [11]. The second weight loss period occurred from 370°C to 650°C, the third period started at 650°C and finished at 750°C corresponding to the weight loss of 11.051% and 5.197%, respectively. This was due to the heat absorption of complete decomposition of FeOOH and $La(OH)_3$ to form corresponding oxides. From about 750°C, it could be observed that the weight of sample was unchanged with respect to the formation of single $LaFeO_3$ phase. It is notable that the exothermic

effect for the phase transformation of $LaFeO_3$, which forms the corresponding oxides, was not observed. This can be explained by the thermal compensation occurring when $LaFeO_3$ transformed from amorphous to crystalline nano-phase. A similar phenomenon was described in [17, 19].

From the results of TGA analysis, the calcination temperatures of 750, 850 and 950°C were chosen to study the formation of single phase $LaFeO_3$. Fig. 2 shows the XRD $LaFeO_3$ pattern of samples after calcination at 750, 850 and 950°C for 1 h.

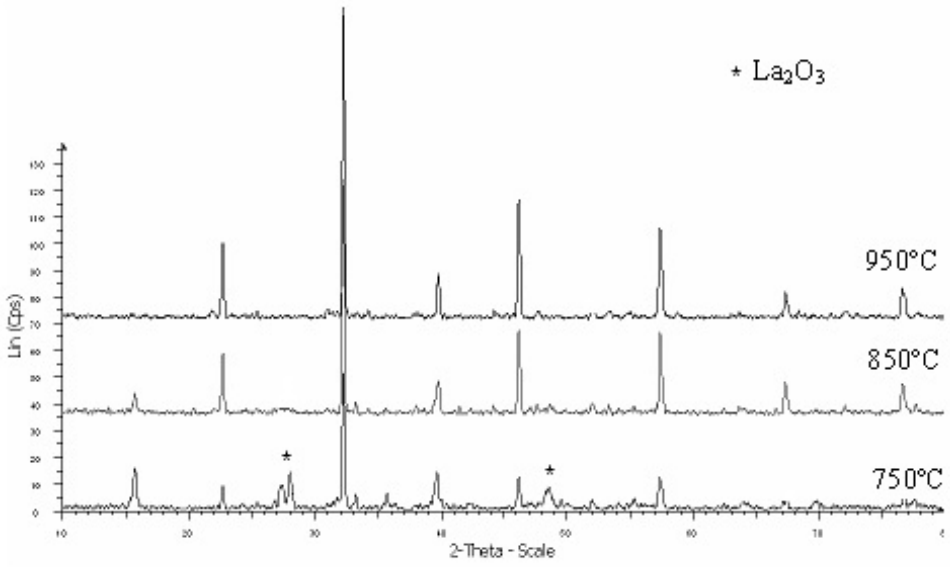

FIG. 2. XRD pattern of $LaFeO_3$ sample heated for 1 h

In the XRD pattern, the typical peaks of single phase of crystalline perovskite $LaFeO_3$ were observed. It can be inferred that the crystallization is almost completed at 750°C, there were only 2 peaks with low intensity at 750°C. At 850°C and 950°C peaks of impurity were not observed.

The result of scanning electron microscope (SEM) of the samples after calcination at 850°C (t = 1 h) shows that the particles exhibit spherical or oval shapes (Fig. 3) with two ranges of size: small particles with a size from 50 to 70 nm, and large particles with a size of about 100 nm or larger. Additionally, it is also demonstrated in the SEM images that the particles bound together to form bulks of particles. This is the limitation of synthesized metal oxides, and particularly $LaFeO_3$, using the co-precipitation method.

As a result, the $LaFeO_3$ material with a particle size of 100 nm was synthesized via the co-precipitation of metal cations Fe^{3+} and La^{3+} in boiling water with aqueous ammonia as co-precipitating agent and calcination temperature of 850°C.

3.2. $La_{1-x}Sr_xFeO_3$ nano-materials synthesis results (x=0.1; 0.2; 0.3)

Because of the high solubility product of $Sr(OH)_2$ (Ts = $3.2x10^{-4}$ at 20°C) [20], and the small solubility product of $Fe(OH)_3$ and $La(OH)_3$ at the same temperature ($3.8x10^{-38}$ and $1.05x10^{-21}$ respectively) [20], it was not possible to co-precipitate La^{3+}, Sr^{2+} and Fe^{3+} cations by aqueous ammonia. Therefore, co-precipitating agent was replaced by ammonium carbonate. The results obtained from experiments of $La_{1-x}Sr_xFeO_3$ (x = 0.1, 0.2, 0.3) synthesis are presented in the section 2.

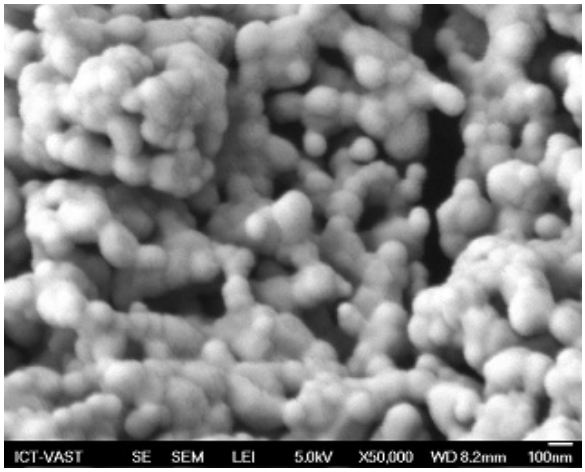

FIG. 3. SEM picture of $LaFeO_3$ sample heated at 850°C (t=1 h)

From the TGA results of synthesized $LaFeO_3$ powders (see Fig. 1), we chose samples with calcination temperatures at 750°C, 850°C and 950°C for 1 h to investigate the formation of single $La_{1-x}Sr_xFeO_3$ phase.

Figure 4, 5, 6 present the XRD patterns of $La_{1-x}Sr_xFeO_3$ materials (x = 0.1, 0.2, 0.3) after calcination at temperatures of 750°C, 850°C and 950°C for 1 h. Figures 4, 5, 6 shows that the obtained products had composition of orthorhombic $LaFeO_3$ phase.

However, the lattice spacing (d) of synthesized crystalline samples decreased with increasing x values (table 1). This could be explained by the replacement of La^{3+} ions by Sr^{2+} ions that led to the lattice shrinkage, therefore the lattice spacing (d) decreased when the Sr^{2+} concentration increased. Indeed, the ionic radius of Sr^{2+} (0.126 nm) is much larger than that of La^{3+} (0.104 nm) [21]. Hence, when La^{3+} ions were replaced by Sr^{2+} ions, charge compensation occurred in the crystalline lattice; consequently, Fe^{3+} ions with a radius of 0.0645 nm were oxidized to Fe^{4+} with a smaller radius (0.0585 nm) [20], thus the lattice spacing (d) decreased. Additionally, the characteristic peaks of lanthanum or strontium phases ($La(OH)_3$, La_2O_3, $La_2(CO_3)_3$, SrO, or $SrCO_3$) were not observed on the XRD pattern. The absence of diffraction peaks for lanthanum and strontium suggested the alloying of strontium in the crystalline lattice of $LaFeO_3$.

Elemental composition of the samples was determined by energy-dispersive X-ray spectroscopy and atomic absorption spectroscopy, indicating that atomic weight percentage of elements in the samples was equal to their stoichiometric percentages. The calculated errors were from 0.7% to 3.5% for samples synthesized by both methods. This could be attributed to the insufficiency of oxygen when replacing La^{3+} by Sr^{2+} in the crystalline lattice.

A study of $La_{0.8}Sr_{0.2}FeO_3$ and $La_{0.7}Sr_{0.3}FeO_3$ materials by scanning electron microscopy (SEM) showed that the formed crystals had an average particle size of about 80–100 nm but it was demonstrated that the differentiation of particles shapes was more obvious as compared to the pure $LaFeO_3$. This once again confirmed that Sr^{2+} doping can affect the structure of the $LaFeO_3$ crystalline lattice.

As a result, Sr doping in the $LaFeO_3$ crystal can lead to a change in the lattice structure, particularly in decreased lattice spacing (d) and the alteration of the crystal shape with increased Sr concentration. This can provide a change in magnetic characteristics of doping $La_{1-x}Sr_xFeO_3$ as compared to pure $LaFeO_3$.

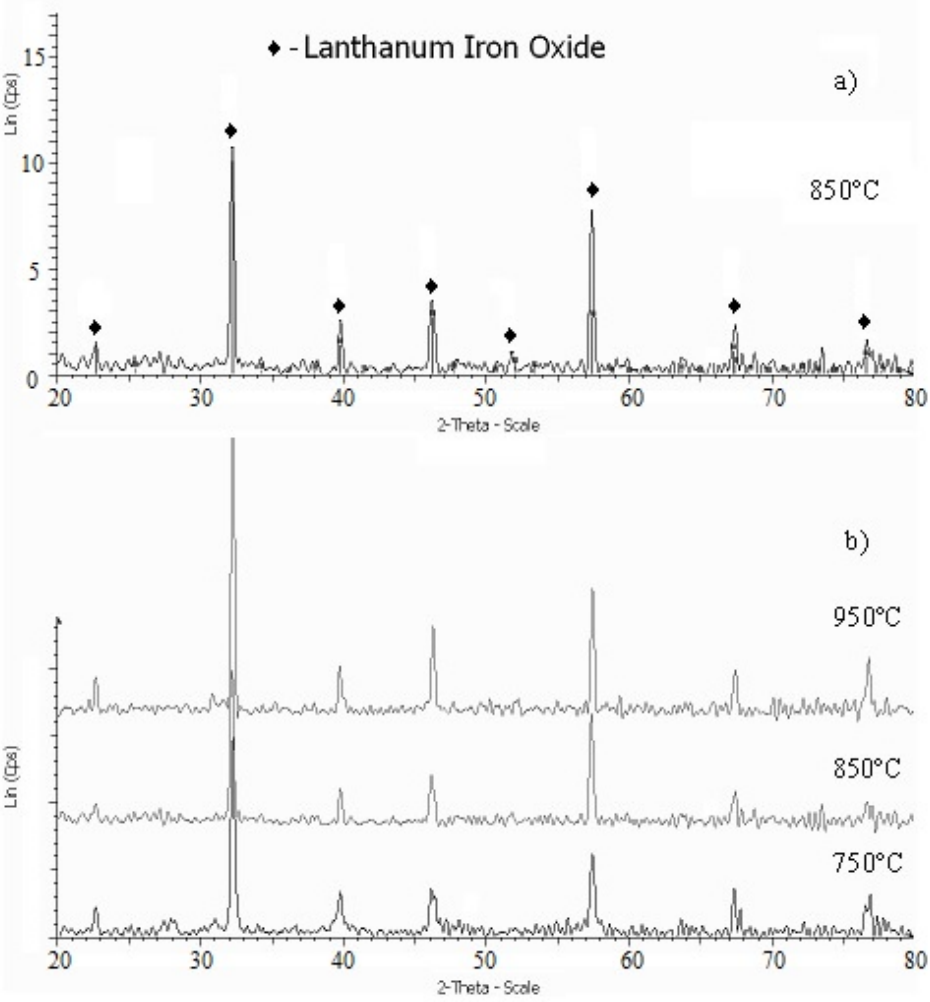

FIG. 4. XRD pattern of $La_{0.9}Sr_{0.1}FeO_3$ sample heated at 850°C (a) and stack XRD diagram of $La_{0.9}Sr_{0.1}FeO_3$ heated at 750°C, 850°C and 950°C (b) (t=1 h)

TABLE 1. The comparison of lattice spacing (d) of $La_{1-x}Sr_xFeO_3$ (x=0.1; 0.2; 0.3) samples heated at 850°C (t=1 h) (from XRD results, Fig. 5, 6, 7)

No	Lattice spacing d; $\AA$		
	$La_{0.9}Sr_{0.1}FeO_3$	$La_{0.8}Sr_{0.2}FeO_3$	$La_{0.7}Sr_{0.3}FeO_3$
1	3.93402	3.91905	3.91813
2	2.78176	2.77718	2.76904
3	2.26766	2.26596	2.26330
4	1.96576	1.96266	1.95876
5	1.76393	1.75545	1.75545
6	1.60434	1.60262	1.60062
7	1.38814	1.38427	1.38427
8	1.24208	1.24057	1.24020

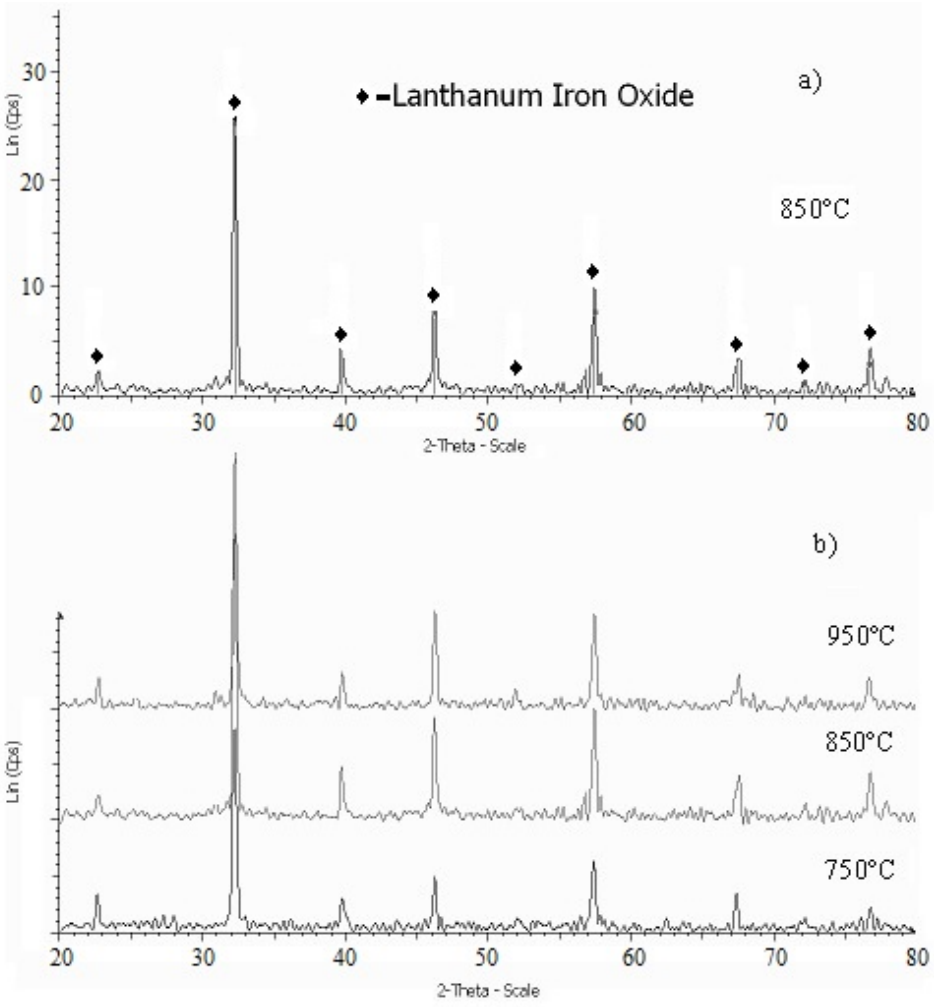

FIG. 5. XRD pattern of $La_{0.8}Sr_{0.2}FeO_3$ sample heated at 850°C (a) stack XRD diagram of $La_{0.8}Sr_{0.2}FeO_3$ heated at 750°C, 850°C and 950°C (b) (t=1 h)

3.3. Magnetic characteristics of $La_{1-x}Sr_xFeO_3$ nanomaterial (x=0.0; 0.1; 0.2; 0.3)

Study of the magnetic properties of nano $La_{1-x}Sr_xFeO_3$ materials (x = 0.0, 0.1, 0.2, 0.3) calcined at 850°C (t=1 hour) on vibrating sample magnetometers at room temperature indicated that the Sr^{2+} doping in the $LaFeO_3$ lattice influenced their magnetic properties (Fig. 8 and table 2). Indeed, in a magnetic field of 1273.6 kA/m the magnetic characteristics of the material, such as saturation magnetization (M_s), remanent magnetization (M_r), decreased with x from 0.0 to 0.1, then increased with x from 0.1 to 0.2, then decreased again with x form 0.2 to 0.3. Meanwhile, the value of coercive force (H_c) of all samples was greater than 15.92 kA/m and increased in the order $LaFeO_3 < La_{0.9}Sr_{0.1}FeO_3 < La_{0.8}Sr_{0.2}FeO_3 < La_{0.7}Sr_{0.3}FeO_3$ (where, H_c of $La_{0.7}Sr_{0.3}FeO_3$ was 20 times greater than H_c of pure $LaFeO_3$). This can be explained in that the alloying of Sr^{2+} in the crystal of pure $LaFeO_3$ increased the non-directionality in shape and crystal lattice of the synthesized materials. Therefore, the synthesized $La_{1-x}Sr_xFeO_3$ samples are hard magnetic materials ($H_c > 7.96$ kA/m).

The regular change in $M_s$and M_r values calculated for $La_{1-x}Sr_xFeO_3$ material with the increasing of Sr^{2+} concentration in the $LaFeO_3$ crystal lattice was due to structure disordering when replacing La^{3+} by Sr^{2+} in the $LaFeO_3$ lattice, which caused the poor orientation of

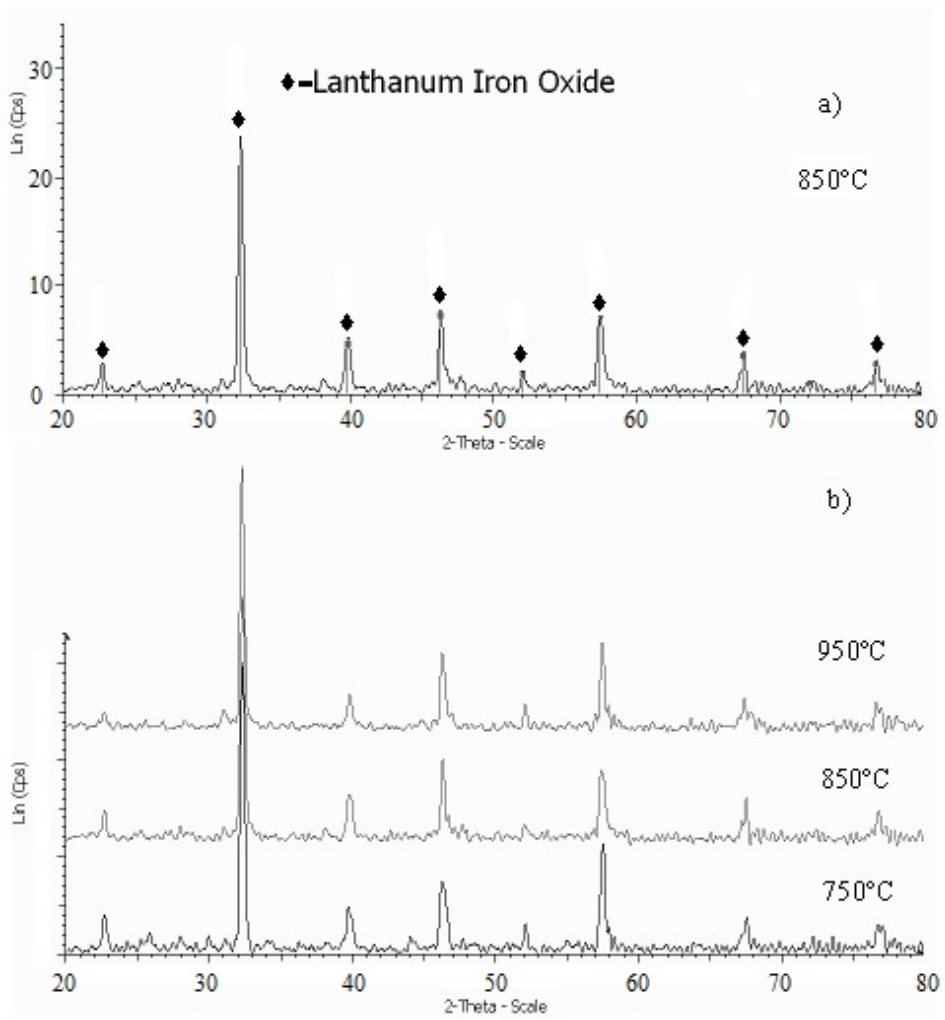

FIG. 6. XRD pattern of $La_{0.7}Sr_{0.3}FeO_3$ sample heated at 850°C (a) and stack XRD diagram of $La_{0.7}Sr_{0.3}FeO_3$ heated 750°C, 850°C and 950°C (b) (t=1 h)

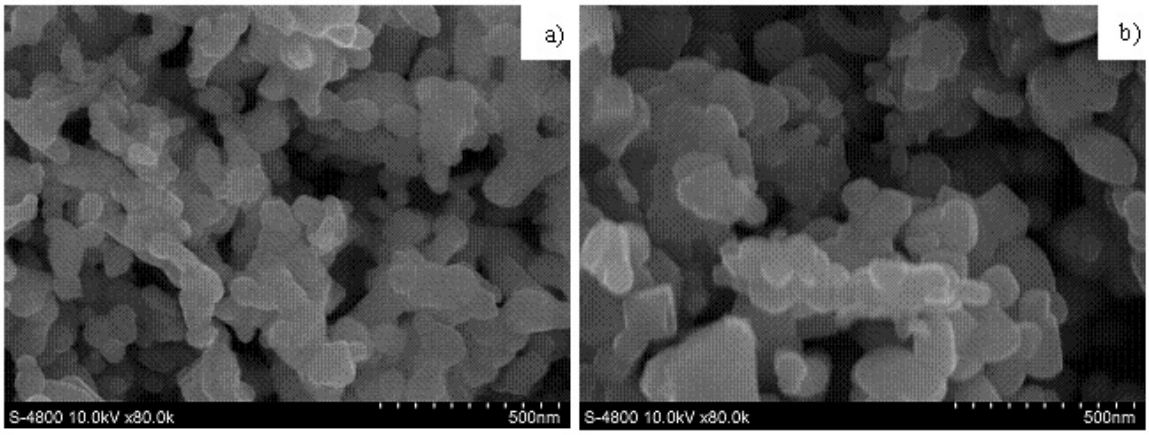

FIG. 7. SEM images of $La_{0.8}Sr_{0.2}FeO_3$ sample (a) and $La_{0.7}Sr_{0.3}FeO_3$ (b) heated at 850°C (t=1 h)

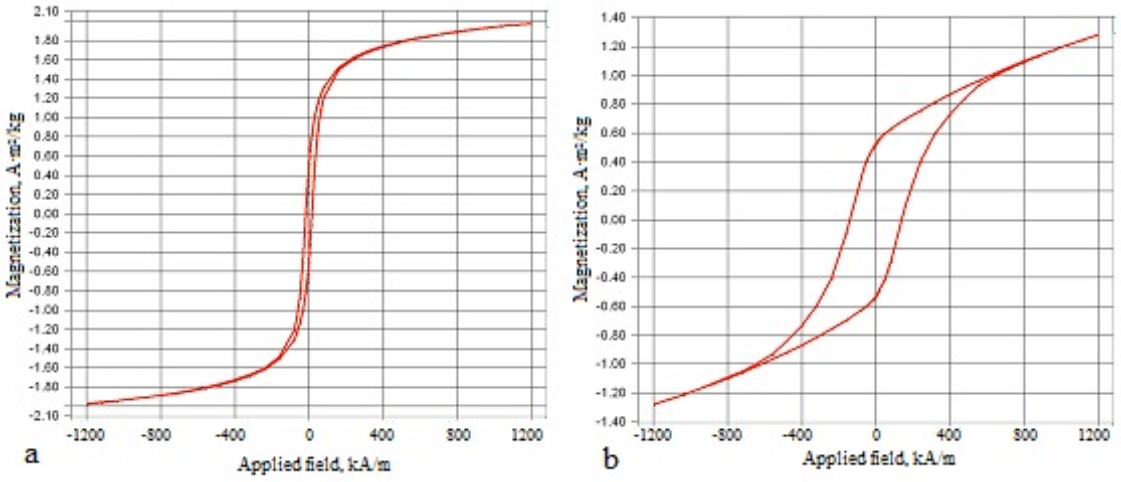

FIG. 8. Magnetic hysteresis loop of $LaFeO_3$ (a) and $La_{0.8}Sr_{0.2}FeO_3$ (b) materials heated at 850°C (t=1 h)

magnetic iron, because of the change in the Fe–O–Fe angle with x from 0.0 to 0.1. With the addition of Sr^{2+} to the crystal lattice to concentration of 20%, the crystalline structure became stabilized and therefore, the M_s and M_r values increased. However, the further addition of Sr^{2+} to the x value of 0.3 could lead to the over-replacement of La^{3+} (trivalent) by Sr^{2+} (divalent). With respect to the charge compensation, some Fe^{3+} ions were oxidized to Fe^{4+} ions (the similar phenomenon was observed in the $Bi_{1-x}Sr_xFeO_3$ [16]). This resulted in the appearance of the magnetic exchange interaction between Fe^{3+} and Fe^{4+} ions through O^{2-} (Fe^{3+}–O^{2-}–Fe^{4+}), leading to a change in the magnetic properties of the synthesized materials.

TABLE 2. Magnetic characteristics of $La_{1-x}Sr_xFeO_3$ nanomaterial (x=0.0; 0.1; 0.2; 0.3) heated at 850°C (t=1h)

Charateristics		$LaFeO_3$	$La_{0.9}Sr_{0.1}FeO_3$	$La_{0.8}Sr_{0.2}FeO_3$	$La_{0.7}Sr_{0.3}FeO_3$
M_r, Am^2/kg	Remanent Magnetization: M at H=0	0.510	0.085	0.527	0.104
M_s, Am^2/kg	Saturation Magnetization: maximum M measured	1.974	0.220	1.278	0.572
H_c, kA/m	Coercive Field: Field at which M/H changes sign	16.183	28.490	138.928	336.952

4. Conclusions

Powders of $La_{1-x}Sr_xFeO_3$ (x = 0.0, 0.1, 0.2, 0.3) with a particle size of about 100 nm was synthesized from La^{3+}, Sr^{2+} and Fe^{3+} cations in heated water by co-precipitation method with ammonia and ammonium carbonate as precipitating agents and a calcination temperature of 750°C (t=1 h). The increase of Sr^{2+} concentration provided to the increase of coercive force of synthesized $La_{1-x}Sr_xFeO_3$ material. The obtained $La_{1-x}Sr_xFeO_3$ nanomaterial showed high coercive force ($H_c > 15.92$ kA/m), hence it was related to the hard magnetic materials and could be used to produce permanent magnets for motors.

Acknowledgments

This work was supported by the Ministry of Education and Science of the Russian Federation in line with government order for Higher Education Institutions in the field of science for 2014-2016 years (project N 225).

References

[1] Rusanov A.I. Striking world of nanostructures. *Russian Journal of General Chemistry*, **72**(4), P. 495–511 (2002).

[2] Popkov V.I., Almjasheva O.V. Yttrium orthoferrite $YFeO_3$ nanopowders formation under glycine-nitrate combustion conditions. *Russian Journal of Applied Chemistry*, **87**(2), P. 167–171 (2014).

[3] Khetre S.M., Jadhav H.V., Jagadale P.N., Kulal S.R., Bamane S.R. Studies on electrical and dielectric properties of $LaFeO_3$. *Journal of Applied Sciences Research*, **2**(4), P. 503–511 (2011).

[4] Wang J., Dong X., Qu Z., Liu G., Yu W. Electrospinning preparation of $LaFeO_3$ nanofibers. *Modern Applied Science*, **3**(9), P. 65–71 (2009).

[5] Cao X., Kim Ch.-S., Yoo H.-I. Effect of substitution of manganese for iron on the structure and electrical properties of yttrium ferrite. *Journal of the American Ceramic Society*, **84**(6), P. 1265–1272 (2001).

[6] Nguyen A.T., Almjasheva O.V., Mittova I.Ya., Stognei O.V., Soldatenko S.A. Synthesis and magnetic properties of $YFeO_3$ nanocrystals. *Russian Journal of Inorganic Materials*, **45**(11), P. 1304–1308 (2009).

[7] Nguyen A.T., Mittova I.Ya., Al'myasheva O.V. Influence of the synthesis conditions on the particle size and morphology of yttrium orthoferrite obtained from aqueous solutions. *Russian Journal of Applied Chemistry*, **82**(11), P. 1915–1918 (2009).

[8] Morozov M.I., Lomanova N.A., Gusarov V.V. Specific features of $BiFeO_3$ formation in a mixture of bismuth(III) and iron(III) oxides. *Russian Journal of General Chemistry*, **73**(11), P. 1772–1776 (2003).

[9] Lomanova N.A., Gusarov V.V. Effect of surface melting on the formation and growth of nanocrystals in the Bi_2O_3-Fe_2O_3 system. *Russian Journal of General Chemistry*, **83**(12), P. 2251–2253 (2013).

[10] Lomanova N.A., Gusarov V.V. Influence of synthesis temperature on $BiFeO_3$ nanoparticles formation. *Nanosystems: Physics, Chemistry, Mathematics*, **4**(5), P. 696–705 (2013).

[11] Nguyen A.T., Mittova I.Ya., Almjasheva O.V., Kirillova S.A., Gusarov V.V. Influence of the preparation conditions on the size and morphology of nanocrystalline lanthanum orthoferrite. *Glass Physics and Chemistry*. **34**(6), P. 756–761 (2008).

[12] Peter S.D., Garbowski E., Perrichon V., Primet M. NO reduction by CO over aluminate-supported perovskites. *Catalysis Letters*, **70**(1-2), P. 27–33 (2000).

[13] Stathopoulos V.N., Belessi V.C., Ladavos A.K. Samarium based high surface area perovskite type oxides $SmFe_{1-x}AlxO_3$ (x= 0.00, 0.50, 0.95). Part II, catalytic combustion of CH_4. *Reaction Kinetics and Catalysis Letters*, **72**(1), P. 49–55 (2001).

[14] Dinh V.T., Mittova V.O., Almjasheva O.V., Mittova I.Ya. Synthesis and magnetic properties of nanocrystalline $Y_{1-x}Cd_xFeO_{3-\delta}$ ($0 \leqslant x \leqslant 0.2$). *Russian Journal of Inorganic Materials*, **47**(10), P. 1141–1146 (2011).

[15] Nguyen A.T., Mittova I.Ya., Solodukhin D.O., Al'myasheva O.V., Mittova V.O., Demidova S.Yu. Sol-Gel Formation and Properties of Nanocrystals of Solid Solutions $Y_{1-x}Ca_xFeO_3$. *Russian Journal of Inorganic Chemistry*, **59**(2), P. 40–45 (2014).

[16] Golubeva O.Yu., Gusarov V.V., Semenov V.G., Volodin V.S. Structural stabilization of Fe^{4+} ions in perovskite-like phases based on the $BiFeO_3$-$SrFeO_y$ system. *Glass Physics and Chemistry*, **35**(3), P. 313–319 (2009).

[17] Oanh P.T.H., Ngoc T.M., Tuyen T.N. Synthesis and electrical properties of materials $La_{1-x}Mn_x$xSrO_3 by the precipitation method. *Vietnam Journal of Chemistry*, **49**(3A), P. 240–245 (2011).

[18] Abdulaziz A.F., Khaleel K.I., Bakr N.A.. Magnetic and magnetostrictive properties of $Co_{1-x}Zn_xFe_2O_4$ nanoparticles produced by co-precipitation method. *Tikrit Journal of Pure Science*, **16**(4), P. 216–222 (2011).

[19] Schweitzer G.K., Pesterfield L.L. *The Aqueous Chemistry of the Elements*. Oxford: OUP, 448 p. (2010).

[20] Richens D.T. *The Chemistry of Aqua Ions*. Wiley, 604 p. (1997).

[21] Sharikov F.Yu., Almjasheva O.V., Gusarov V.V. Thermal analysis of formation of ZrO_2 nanoparticles under hydrothermal. *Russian Journal of Inorganic Chemistry*, **51**(10), P. 1538–1542 (2006).

[22] Lide R.D. *Handbook of Chemistry and Physics*, 84-th Edition. Copyright CRC Press LLC, 2475 p. (2004).

[23] Shannon R.D. Revised effective ionic radii and systematic studies of interatomic distances in halides and chalcogenides. *Acta Crystallographica. Section A*, **32**(5), P. 751–767 (1976).